Journal of Organometallic Chemistry, 378 (1989) 255–277
Elsevier Sequoia S.A., Lausanne – Printed in The Netherlands
JOM 20200

Variable temperature ^{1}H NMR studies of [M(COD)(μ-L)]$_2$ (M = Rh, Ir; L = substituted hydroxypyridinate). Facile intramolecular bridging ligand exchange and metal–metal bond cleavage

Gary S. Rodman and Kent R. Mann *

Department of Chemistry, University of Minnesota, Minneapolis, MN 55455 (U.S.A.)

(Received April 7th, 1989)

Abstract

The variable temperature ^{1}H NMR spectra of [M(COD)(μ-L)]$_2$ (M = Rh, Ir: L = 2-hydroxypyridinate (μ-hp), 6-methyl-2-hydroxypyridinate (mhp)) in toluene-d_8 solutions are described. Our analysis of the ^{1}H NMR spectra indicates that the binuclear hydroxypyridinate complexes undergo fluxional processes significantly different than previously studied mononuclear analogues. Two distinct exchange processes interconvert nonequivalent COD protons in [Rh(COD)(μ-hp)], but only the lower energy process is observed in [Ir(COD)(μ-hp)]$_2$. The resonances of the bridging ligands are essentially unaffected by temperature changes. The low energy process (process 1) interconverts COD hydrogens trans to N with those *trans* to O, but does not interconvert "inside" with "outside" hydrogens. The second process (process 2), observed for [Rh(COD)(μ-hp)]$_2$, interconverts inside with outside protons. Line shape analyses of the variable temperature spectra of the hp complexes yielded the rates and activation parameters of processes 1 and 2. Analogous behavior was observed for [Ir(COD)(μ-mhp)]$_2$ and [Rh(COD)(μ-mhp)]$_2$. No exchange behaviour was observed in the spectrum of the related complex, [Ir(COD)(μ-pz)]$_2$. The effects of concentration, added COD, and added nucleophile (acetonitrile) on the rates of exchange are discussed. "Cross-over" experiments, in which two different [M(COD)(μ-L)]$_2$ species were mixed together, demonstrate that process 1 is strictly intramolecular. The rotation and/or dissociation of COD ligands, the complete dissociation of the bridging ligands and the rupture of the M–M interaction are not involved with process 1. Process 1 must involve only motion of the bridging ligands, and does not involve the formation of mononuclear intermediates. For process 2, dissociation of COD was ruled out, but the rotation of the coordinated diene or the inversion of the 8-membered metallocyclic ring are viable

* To whom correspondence should be addressed.

0022-328X/89/$03.50

mechanisms. Cross-over experiments show that at temperatures where the rate of process 2 is appreciable, metal–metal and bridging ligand exchange occurs. These results, and the large positive entropy of activation of process 2 in $[Rh(COD)(\mu\text{-hp})]_2$ imply a dissociative mechanism. Process 2 has a substantially higher activation barrier in $[Ir(COD)(\mu\text{-hp})]_2$ than in $[Rh(COD)(\mu\text{-hp})]_2$, consistent with the stronger M–M interaction expected for the Ir_2 complex. Both proposed pathways for process 2 involve substantial weakening of the M–M interaction.

Introduction

There have been recent studies [1,2] or a new series of Rh^I and Ir^I complexes of the form $[M(COD)(\mu\text{-L})]_2$ (where M = Rh, Ir; μ-L-2-hydroxpyridinate (μ-hp), 6-methyl-2-hydroxpyridinate (mhp)). In a previous communication [1a] and two full papers [1b,1c], we have reported on the structural characterization of these compounds and pointed out that they may have properties important in excited state multielectron transfer reactions. X-ray crystallography indicates that the compounds are binuclear, with the familiar "open-book" configuration [3]. Through the application of COSY and nOe techniques, it was possible to completely assign the ^1H NMR spectra of the compounds. While studying the ^1H NMR spectra of these compounds [1b], a substantial temperature dependence of the spectra, particularly for M = Rh was observed. The nature of the chemical processes which produce the temperature dependence of the ^1H NMR spectra observed for these compounds has been elucidated and is the subject of this report.

Experimental

General considerations

The syntheses of the compounds used in this study were previously reported [1b]. Samples for the variable temperature NMR studies were prepared as follows: A weighed quantity of complex was placed in a dry NMR tube. The tube was attached to a vacuum line through a "tip off manifold" (Ace Glass Inc.) and evacuated. The NMR solvent (toluene-d_8 Aldrich)) was degassed (four freeze-pump-thaw cycles) and distilled into the NMR tube up to a mark (previously determined by filling with water) indicating a 0.50 ml volume. The tubes were then sealed with a torch.

The 300 MHz ^1H and 75.5 MHz ^{13}C NMR spectra were obtained on a Nicolet NT-300 spectrometer. Chemical shifts were referenced to the residual proton o carbon signals from the solvent. The following values were used: ^1H NMR, 2.09 for the methyl resonance of toluene-d_8, 2.00 for the methyl resonance of *ortho*-xylene-d_{10}; ^{13}C NMR, 20.4 for the methyl resonance of toluene-d_8. All shifts are reported in δ (ppm).

Temperature control of the NMR probe was achieved using a TRI Research T-200 Cryo Controller, which regulated the heating of a liquid N_2 cooled N_2 stream directed at the sample. Probe temperatures were determined by replacing the sample with tubes containing methanol (0.3% HCl) for low temperature measurements and ethylene glycol (0.03% HCl) for high temperature measurements and using the equations of Van Geet adjusted to 300 MHz [4]. Temperature measurements were

taken before and after each sample measurement to insure temperature stability. The precision of the temperature measurements is estimated to be ± 1 K.

Dynamic NMR spectra were simulated with DYNAMAR, a program written for intramolecular exchange by Dr. P.Z. Meakin [5] of duPont de Nemours, Inc. The Program had been modified by Prof. S.T. McKenna at the University of California, Berkeley, and by Dr. Richard A. Newmark of 3M, Inc. to automatically vary the exchange rate to fit either a line width or valley between two peaks. The calculations were carried out on a DEC VAX 11/780 computer. A subroutine was written to plot the calculated spectra (1000 points each) on a CRT using the Tektronix PLOT 10 graphics package available on the VAX computer. The final simulated spectra were transferred to a Zenith 150 microcomputer and plotted on a Hewlett–Packard 7470A digital plotter using Lotus 1–2–3 software. The experimental spectra were then replotted to the scale of the simulations.

The temperature dependence of the chemical shifts in the absence of chemical exchange was established from spectra in which line broadening did not occur. A linear dependence of the chemical shift with $1/T$ was observed. Chemical shifts that were corrected for temperature dependence in the absence of chemical exchange were employed in the simulation program. The observed linewidths and peak/valley ratios were measured by hand using expanded plots of the NMR data.

Free energies of activation were calculated from absolute rate theory:

$$k = (k_b T/h) \exp(-\Delta G^{\ddagger}/RT) \tag{1}$$

Where k is the first order rate constant derived from the spectral simulation at T, $\Delta G^{\ddagger}$ is the Gibbs free energy of activation, and k_b, h, R, and T have the usual meanings. Least-squares fits to the equation:

$$\Delta G^{\ddagger} = \Delta H^{\ddagger} - T\Delta S^{\ddagger} \tag{2}$$

gave the free enthalpies and entropies of activation. In the cases where two fluxional processes were clearly discernable (Rh_2 complexes), the NMR data were fit with two rate constants. Because the computer program allowed iteration of only one rate constant, the rate of the lower energy process was estimated at temperatures where the second rate constant was significant by extrapolation of the lower temperature data with eq. 2, where $\Delta G^{\ddagger}$ was linear with T.

Permutation analysis

The analysis of the dynamic NMR data with the program DYNAMAR uses a "jump model", which gives information concerning the permutation which interconverts an initial labeled nuclear configuration to the configuration after rearrangement. As usual, no direct mechanistic information is obtained in this model to indicate the actual physical path involved [5]. In the case of all the hydroxypyridinate complexes studied here, the twelve protons on a given COD ligand can be divided into the three sets containing four protons each: the olefinic protons, the *exo*-methylene protons, and the *endo*-methylene protons (Fig. 1). Interconversions between protons in different sets are never observed (vide infra). Therefore, each set may be analyzed separately, with each group undergoing the same fluxional process, giving the same rate constant. Because each set contains four nuclei, there are $4! = 24$ possible permutations by which the initial labeled configuration can be rearranged (permutation group S_4). King [6] has considered the symmetries of

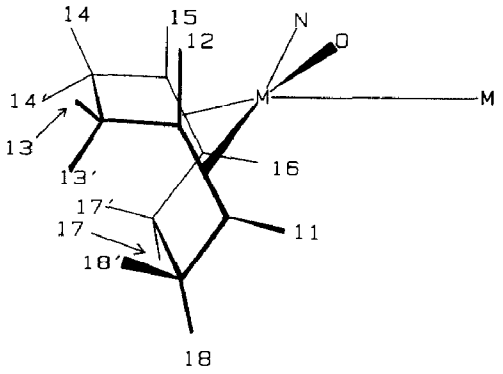

Fig. 1. COD ligand labelling scheme.

permutation groups of order S_n. The full analysis of permutation group S_4 applied to the olefinic protons is shown in Table 1, derived by Bonnaire et al. to analyze the possible permutations for the COD ligands in $[(Rh(COD))_2(salophen)]$ [7]. (The atoms inside a particular set of parentheses interconvert.) In our case, because all COD protons are inequivalent, no simplifications based on symmetry are possible. As pointed out by Bonnaire et al. [7], only permutation set V is applicable to the COD ligands, as sets II, III, and IV would destroy the COD moiety (set I is the trivial identity operation). An identical analysis applies to the sets of *exo*- and *endo*-methylene protons, with the appropriate atomic label substitutions. (See Fig. 1 for labelling scheme.)

An additional complication not present in the mononuclear case arises in the binuclear case. This involves the possibility of a process that exchanges the COD attached to M1 with the one attached to M2. Taking this into consideration requires a more complex permutation analysis. However, because both COD ligands are

Table 1

Permutation analysis of olefinic COD protons in $[M(COD)(\mu\text{-}L)]_2$, L = bidentate ligand with C_s symmetry

Basic permutation set	Permutation [a]		Comment
I: $1x_1^4$	(11)(12)(15)(16)		Identity
II: $8x_1x_3$	(11)(12,16,15)	(11)(12,15,16)	
	(12)(15,16,11)	(12)(16,15,11)	
	(15)(16,12,11)	(15)(16,11,12)	Impossible
	(16)(11,12,15)	(16)(11,15,12)	
III: $6x_1^2x_2$	(11)(12)(15,16)	(11)(15)(12,16)	
	(11)(16)(12,15)	(12)(15)(11,16)	Impossible
	(12)(16)(11,15)	(15)(16)(11,12)	
IV: $6x^4$	(15,12,16,11)	(16,15,12,11)	
	(12,16,15,11)	(11,15,16,12)	Impossible
	(15,16,11,12)	(11,16,12,15)	
V: $3x_2^2$	(12,11)(16,15)		
	(15,11)(16,12)		Possible
	(16,11)(15,12)		

[a] Numbers refer to atomic labeling scheme of Fig. 1.

chemically equivalent in the case studied here, the additional spectral changes produced by interconverting the COD ligands from one metal to the other are indistinguishable from permutations 1 through 4. Thus, permutational arguments still need only consider permutation set V from Table 1.

Results

Variable temperature ^1H NMR spectrum of [Ir(COD)(μ-hp)]$_2$

Figure 2 shows the ^{1}H NMR spectrum of [Ir(COD)(μ-hp)]$_2$ between 291 and 387 K. Note that aside from slight temperature induced chemical shifts, the spectrum of the hp region (ca. 6.2–8.0 ppm) is not significantly affected over the temperature range studied. At high temperatures, the four olefinic resonances H11, H12, H15, and H16 appear to coalesce to a single broad signal at ca. 4.10 ppm. Although this broad signal is within 26 Hz of the average chemical shift calculated for 387 K in the absence of exchange, a single, fluxional process that interconverts all four olefinic protons is ruled out by examination of the methylene region (1.0–3.0 ppm) of the spectrum.

The four signals due to the *exo*-methylene protons H17, H13, H18, and H14 undergo a pairwise interconversion and collapse into two sets of resonances at 387 K. Noting the overlap of the H13 and H18 signals, the pairs of *exo*-methylene protons that interconvert are H17 with H13 or H18 and H14 with H13 or H18. Taking into account the previous, unambiguous assignment of these resonances [1b], this result demonstrates that a COD proton *trans* to N exchanges with one *trans* to O, but leaves unresolved whether or not there is inside–outside exchange.

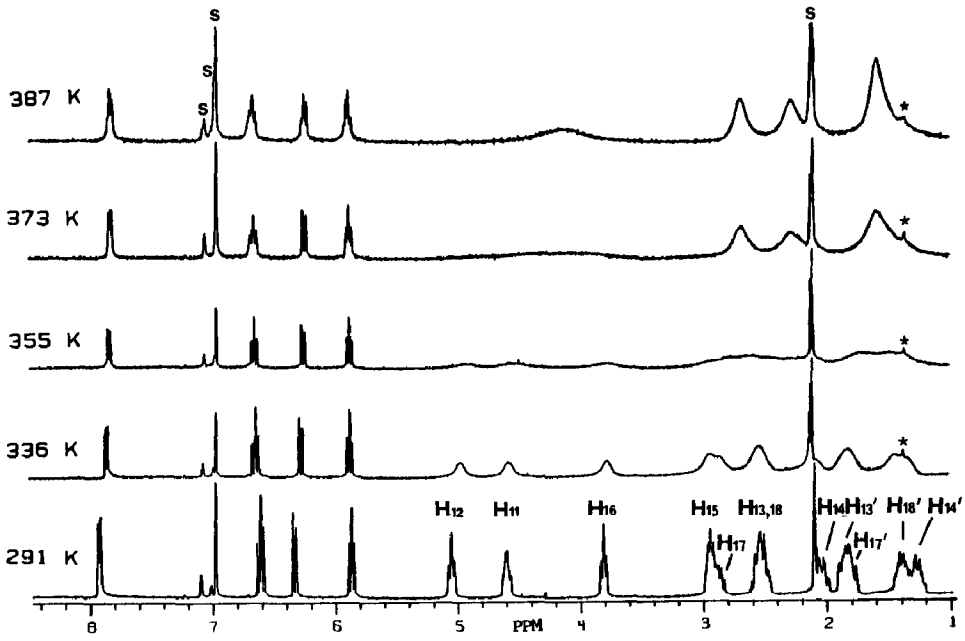

Fig. 2. Variable temperature ^{1}H NMR spectra of [Ir(COD)(μ-hp)]$_2$ in toluene-d_8. s indicates solvent resonances, and ★ indicates a solvent impurity.

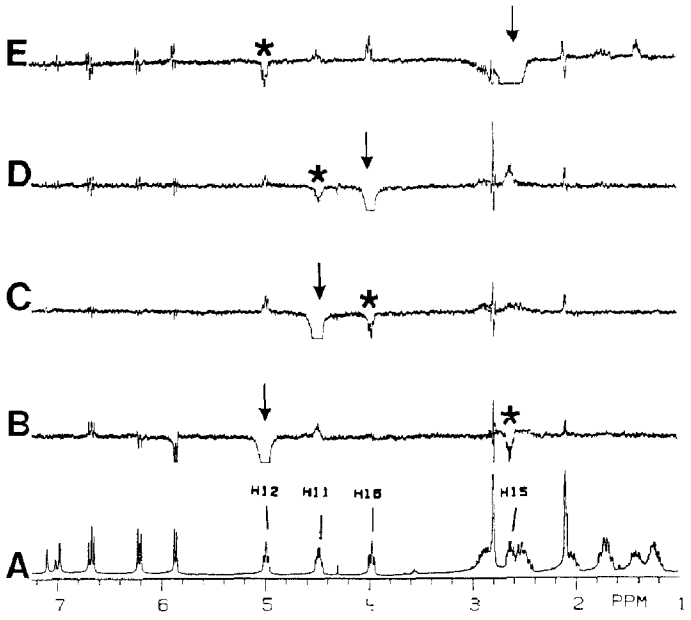

Fig. 3. NOE experiments with $[Ir(COD)(\mu\text{-mhp})]_2$ in toluene-d_8 at 298 K. (A) Reference spectrum. (B) Difference spectrum obtained upon irradiating H12 resonance. (C) Difference spectrum obtained upon irradiating H11 resonance. (D) Difference spectrum obtained upon irradiating H16 resonance. (E) Difference spectrum obtained upon irradiating H15 resonance. Arrows indicate irradiated resonances, while stars indicate resonances that experience negative NOE.

The four signals due to the *endo*-methylene protons H13′, H17′, H18′, and H14′ collapse into a broad signal at ca. 1.7 ppm with a perceptible shoulder at ca. 1.65 ppm. When combined with the conclusions based on the exo methylene region, the collapse of the *endo*-methylene region is consistent only with a process that does not exchange outside with inside COD protons. For example, H18′ and H14′ do not interconvert. The variable temperature NMR data for this complex can only be explained by a process that interconverts the outside COD protons *trans* to N (H11) with outside COD protons *trans* to O (H16) and likewise for the inside protons (H12 ↔ H15). Further, *exo*-methylene protons do not interconvert with *endo*-methylene protons. These results are summarized in permutation notation as follows: Olefinic protons (11,16)(12,15), *exo*-methylene protons (13,14)(17,18) and *endo*-methylene protons (13′,14′)(17′,18′).

The proposed permutation scheme is in agreement with nOe studies carried out on $[Ir(COD)(\mu\text{-hp})]_2$ and $[Ir(COD)(\mu\text{-mhp})]_2$ under conditions where slow chemical exchange occurs. Figure 3 shows the results of a 298 K nOe study of $[Ir(COD)(\mu\text{-mhp})]_2$ in toluene-d_8. Irradiation of the resonance due to H12 (or H15) leads to negative enhancement of H15 (or H12), while irradiation of H11 (or H16) gives a negative enhancement of H16 (or H11). Chemical exchange (via spin saturation transfer) is the source of the "negative nOe", as verified by an identical experiment carried out at low temperature at the stopped exchange limit, where the negative enhancements are not observed, nOe experiments conducted at a higher (360 K) temperature give significantly larger, negative enhancements than those observed at room temperature.

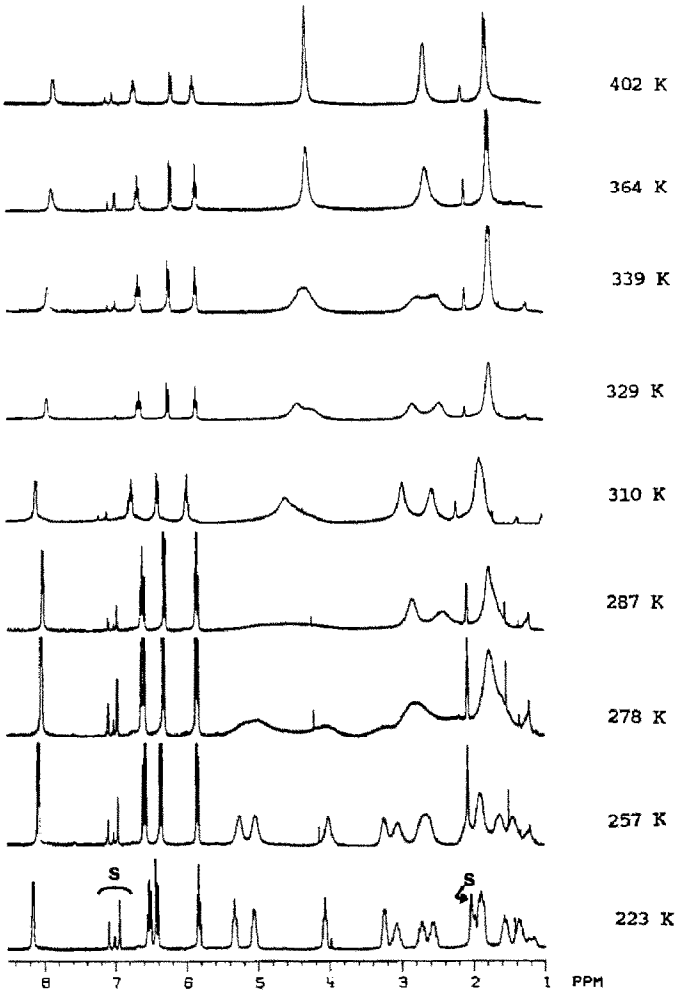

Fig. 4. Variable temperature ^{1}H NMR spectra of [Rh(COD)(μ-hp)]$_2$ in toluene-d_8. s indicates solvent resonances.

Variable temperature ^{1}H NMR spectra of [Rh(COD)(μ-hp)]$_2$

Figure 4 shows the ^{1}H NMR spectrum of [Rh(COD)(μ-hp)]$_2$ between 223 and 402 K in toluene-d_8. The hp region of the spectrum is not significantly affected throughout this temperature range. The spectral changes in the COD region between 223 and 310 K are very similar to those seen in the spectrum of the Ir_2 analogue between 292 and 400 K. In this temperature range, the four olefinic resonances (H11, H12, H15, and H16) coalesce into two broad signals at 4.48 and ca. 4.40 ppm; the four *exo*-methylene signals (H17, H13, H18, and H14) collapse into two signals at 2.84 and 2.44 ppm; and the four *endo*-methylene signals (H13′, H17′, H18′, and H14′) collapse to a broad resonance at 1.78 ppm with a shoulder at ca. 1.74 ppm. The permutations that describe the observed interchange of COD protons in this temperature regime are identical to those of [Ir(COD)(μ-hp)]$_2$ (vide supra).

Between 310 and 402 K, a second fluxional process causes additional collapse of the two olefinic signals observed at 310 K to a single resonance at 2.45 ppm. The two *exo*-methylene signals also collapse to one resonance at 2.62 ppm, and the two

endo-methylene signals coalesce to a single structured resonance at 1.74 ppm ($J_{(ave)}$ 7.96 Hz). These spectral changes are due to the interconversion within the sets of all four olefinic, *exo*-methylene, and *endo*-methylene protons. No interconversion among the two sets of methylene protons is observed. The chemical shifts observed at the high temperature limit are within 3.8, 1.1, and 9.1 Hz of the weighted average of the calculated chemical shifts in the absence of chemical exchange for the olefinic, *exo*-methylene, and *endo*-methylene protons, respectively. The observed coupling constant for the 402 K *endo*-methylene doublet is within 0.35 Hz of the average of all calculated *endo*-methylene coupling constants ($J_{(ave)}$ 8.31 Hz). Thus, between 310 and 402 K, the "inside" and "outside" protons interconvert. In the computer simulation, two permutations are required to account for this process, because the lower energy process removes the distinction between protons *trans* to N and those *trans* to O. The permutations are: Olefinic protons: (11,12)(15,16), (11,15)(12,16); *exo*-methylene protons: (13,17)(14,18),(13,18)(14,17); and *endo*-methylene protons: (13′,17′)(14′,18′),(13′,18′)(14′,17′). The rates of each of the two permutations are exactly half the rate of the actual fluxional process, and the rates are the same for the three sets of protons.

Rate measurements for [Ir(COD)(μ-hp)]$_2$

The olefinic region of the ^{1}H NMR spectrum of [Ir(COD)(hp)]$_2$ (14.0 m*M* in toluene-d_8) was successfully simulated as a function of temperature with the permutation (11,16)(12,15). The spectrum was simulated with six spins, four spins for each of the olefinic protons and two "dummy" spins [8*] to account for the coupling to methylene protons. One dummy spin was given a chemical shift near the average of the four *exo*-methylene resonances, the other was given a chemical shift near the average of the four *endo*-methylene resonances. The coupling constants were taken from the static spectral simulation of [Ir(COD)(μ-hp)]$_2$ [2]. The experimental and simulated spectra are shown in Fig. 5. The spectral changes were fully reversible. The calculated rates and free energies of activation, $\Delta G^{\ddagger}$, are given in Table 2. A plot [9] of $\Delta G^{\ddagger}$ vs. T is linear (corr. coef. = 0.97) and gives a $\Delta H^{\ddagger}$ of 13.5 ± 1 kcal/mol and a $\Delta S^{\ddagger}$ of −10.2 ± 2 e.u.

Rate measurements for [Rh(COD)(μ-hp)]$_2$

The olefinic and *exo*-methylene regions of the ^{1}H NMR spectrum of [Rh(COD)(μ-hp)]$_2$ (7.5 mM in toluene-d_8) were simulated as a function of temperature. In the temperature range between 223 and 299 K, the permutations (11,16)(12,15) (olefinic region) and (13,14)(17,18) (*exo*-methylene region) were used successfully to simulate the spectral changes (Fig. 6a. Above 299 K, the spectra could not be simulated without the inclusion of the second process. Accordingly, the permutations (11,12)(15,16) and (11,15)(12,16) were added to the olefinic proton simulation, and the (13,17)(14,18) and (13,18)(14,17) permutations were added to the *exo*-methylene proton simulation (Fig. 6b). The same six spin approximation was used as in the [Ir(COD)(μ-hp)]$_2$ simulations [10*].

To further confirm the applicability of this model, rates calculated from the simulation of the olefinic region were found to adequately simulate the changes in

* Reference number with asterisk indicates a note in the list of references.

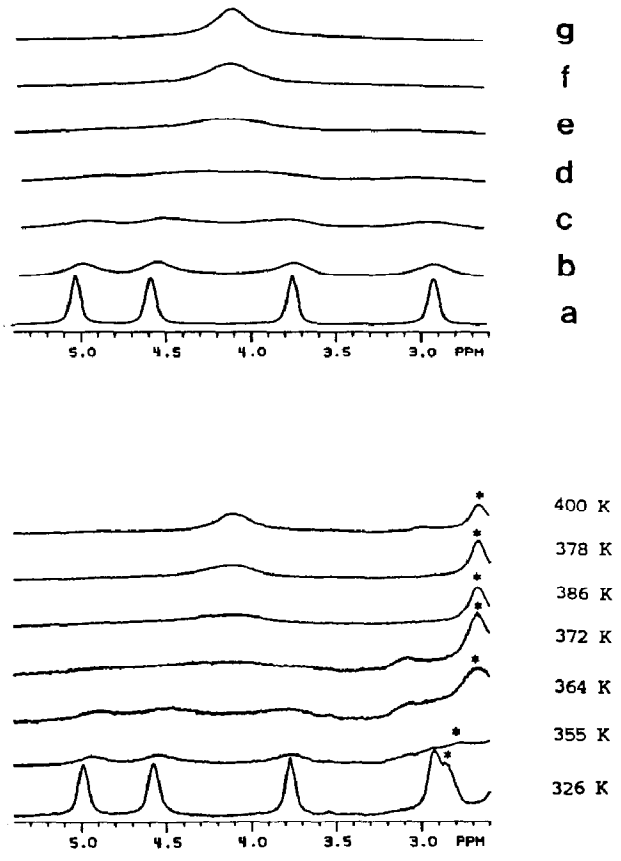

Fig. 5. Observed (lower) and simulated (upper) ^{1}H NMR spectra (olefinic) COD region) of [Ir(COD)(μ-hp)]$_2$ in toluene-d_8. ★ indicates *exo*-methylene resonances not included in this simulation. (a) $k_1 = 33$ s^{-1}; (b) $_1$ 190 s^{-1}; (c) k_1 340 s^{-1}; (d) k_1 550 s^{-1}; (e) k_1 820 s^{-1}; (f) k_1 1300 s^{-1}; (g) k_1 1800 s^{-1}.

the *exo*-methylene region [9]. The calculated rates and free energies of activation ($\Delta G^{\ddagger}$) are given in Table 3. The activation parameters for the lower energy process were obtained from a least-squares fit of $\Delta G^{\ddagger}$ vs. T data between 240 and 312 K (Fig. 7). A linear (corr. coef. = 0.988) fit gave $\Delta H^{\ddagger}$ of 11.1 ± 0.1 kcal/mol and $\Delta S^{\ddagger} = -7.4 \pm 0.4$ e.u. for process one. A least-squares fit of $\Delta G^{\ddagger}$ vs. T data for the

Table 2

Calculated rates and activation energies for proton exchange in [Ir(COD)(μ-hp)]$_2$

T (K)	k (s^{-1})	$\Delta G^{\ddagger}$ (kcal/mol)
218	0	–
292	3	16.4
326	33	16.9
355	190	17.2
364	340	17.2
372	550	17.3
378	820	17.3
386	1300	17.3
400	1800	17.7

second process between 310.5 K and 363.7 K (Fig. 8) was linear (corr. coef. 0.932) and gave $\Delta H^{\ddagger} = 25.3 \pm 1.4$ kcal/mol and $\Delta S^{\ddagger} = +25.9 \pm 4.1$ e.u.

Rate measurements for [M(COD)(μ-mhp)]$_2$ (M = Rh, Ir)

Both complexes display exchange behavior for the COD resonances as a function of temperature that are qualitatively similar to that observed for the hp complexes and the same permutation schemes apply. The broadening and eventual coalescence occurs at somewhat higher temperatures in the mhp complexes, but to determine if the activation energies are significantly different from the hp analogues, spectral simulation is required. In the stopped exchange region, the chemical shift difference between the H15 and H12 (outside olefinic protons) resonances in [Ir(COD)(μ-mhp)]$_2$ is about 0.3 ppm larger than that in [Ir(COD)(μ-hp)]$_2$; therefore faster rates are required for the mhp COD resonances to coalesce. Although we have not simulated the spectra for the mhp complexes, it is apparent that the activation parameters of the mhp compounds are not drastically different from those of the hp complexes.

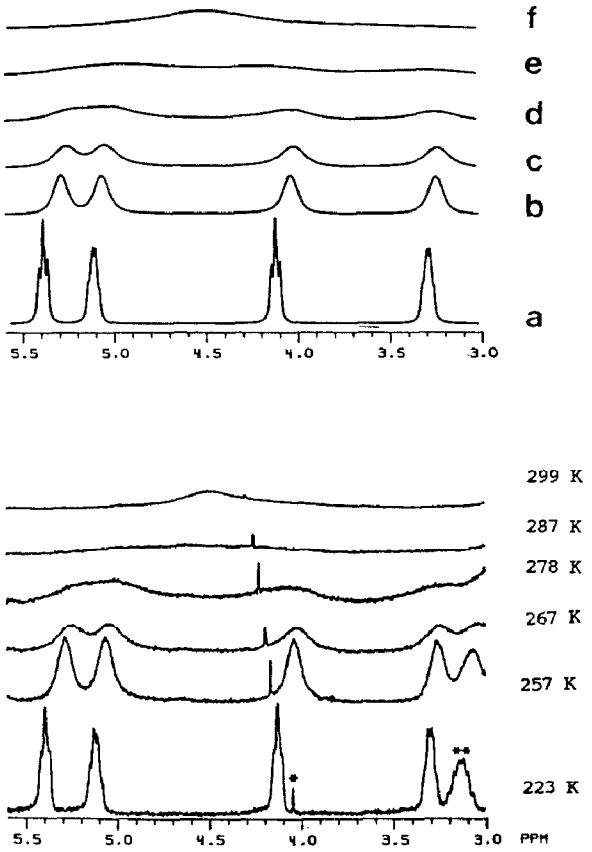

Fig. 6a. Observed (lower) and simulated (upper) ^{1}H NMR spectra (olefinic COD region) of [Rh(COD)(μ-hp)]$_2$ in toluene-d_8 between 310 and 402 K. ★ indicates impurity resonance. ★★ indicates COD resonance not included in this simulation. (a) k_1 0 s^{-1}; (b) k_1 52 s^{-1}; (c) k_1 120 s^{-1}; (d) k_1 280 s^{-1}; (e) k_1 540 s^{-1}; (f) k_1 1200 s^{-1}.

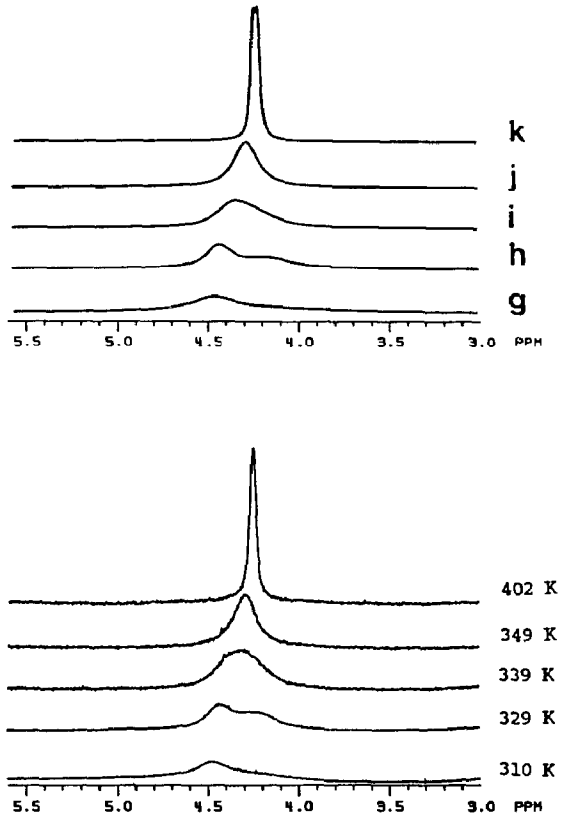

Fig. 6b. Observed (lower) and simulated (upper) ^{1}H NMR spectra (olefinic COD region) of [Rh(COD)(μ-hp)]$_2$ in toluene-d_8 between 310 and 402 K. (g) k_1 2400 s^{-1}, k_2 6.4 s^{-1}; (h) k_1 7300 s^{-1}, k_2 50 s^{-1}; (i) k_1 13000 s^{-1}, k_2 220 s^{-1}; (j) k_1 21000 s^{-1}, k_2 540 s^{-1}; (k) k_1 190000 s^{-1}, k_2 69000 s^{-1}.

Table 3

Calculated rates and activation energies for proton exchange in [Rh(COD)(μ-hp)]$_2$

T (K)	$k(1)$ (s^{-1})	$k(2)$ (s^{-1})	$\Delta G^{\ddagger}(1)$ (kcal/mol)	$\Delta G^{\ddagger}(2)$ (kcal/mol)
223	–	–	–	–
242	12	–	12.9	–
257	52	–	13.0	–
267	120	–	13.0	–
278	280	–	13.1	–
287	540	–	13.2	–
299	1200	0.0	13.3	–
310	2400	6.4	13.4	17.1
320	6000	9.0	13.2	17.4
329	7300 [a]	50	13.5 [a]	16.8
339	13000 [a]	220	13.6 [a]	16.3
349	21000 [a]	540	13.7 [a]	16.2
364	41000 [a]	2000	13.8 [a]	15.9
383	93000 [a]	14000 [a]	13.9 [a]	15.4 [a]
402	190000 [a]	69000 [a]	14.0 [a]	14.9 [a]

[a] Value obtained by extrapolation of lower temperature data.

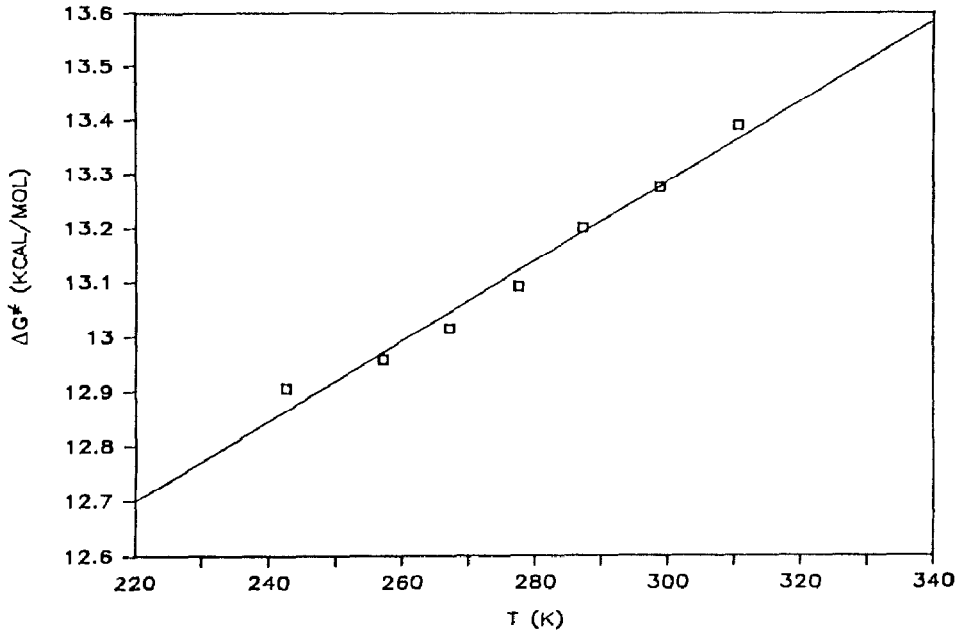

Fig. 7. Plot of $\Delta G^{\ddagger}$ vs. T for proton exchange (process 1) in $[Rh(COD)(\mu\text{-hp})]_2$. Least squares line is drawn with $\Delta H^{\ddagger}$ 11.1 kcal/mol and $\Delta S^{\ddagger}$ −7.4 e.u.

Rate measurements for [M(COD)(8hq)] (M = Rh, Ir)

The ^{1}H NMR spectrum of [Rh(COD)(8hq)] was briefly described by Ugo et al. in 1968 [11]. nOe measurements on this complex and the Ir analogue indicate that both

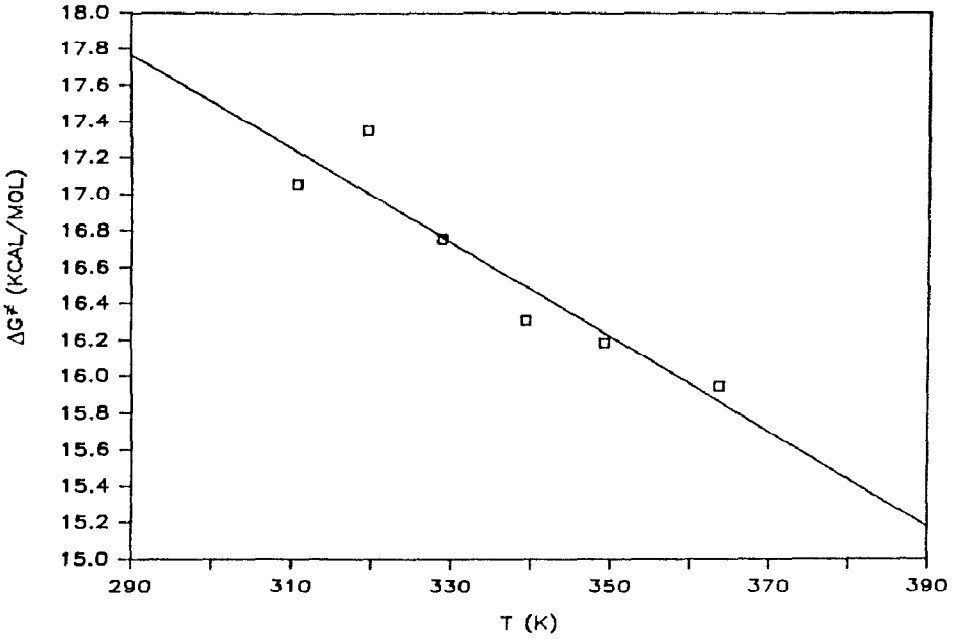

Fig. 8. Plot of$\Delta G^{\ddagger}$ vs. T for proton exchange (process 2) in $[Rh(COD)(\mu\text{-hp})]_2$. Least squares line is drawn with $\Delta H^{\ddagger}$ 25.3 kcal/mol and $\Delta S^{\ddagger}$ 25.9 e.u.

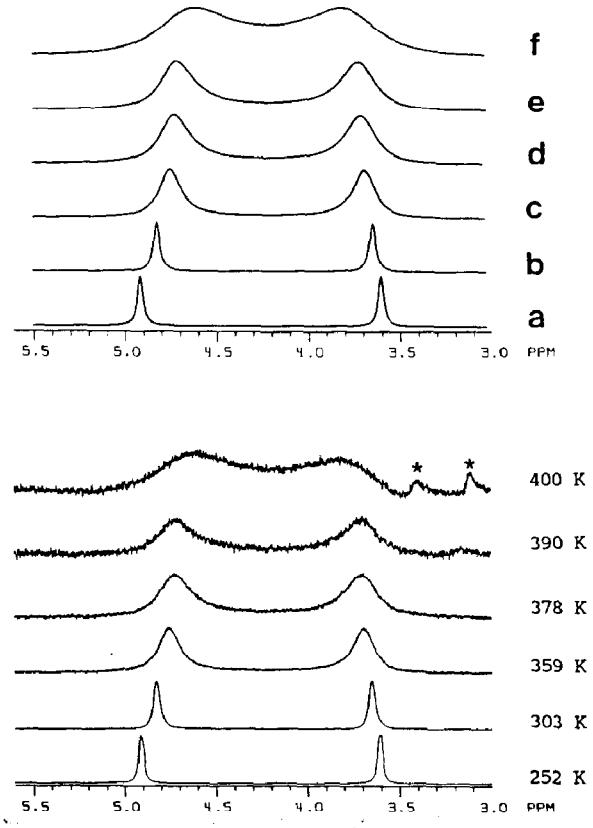

Fig. 9. Observed and simulated ^{1}H NMR spectra (olefinic COD region) of $[Rh(COD)(8hq)]_2$ in *o*-xylene-d_{10}. ★ indicates impurity resonance. (a) k_1 0 s^{-1}; (b) k_1 6 s^{-1}; (c) k_1 99 s^{-1}; (d) k_1 150 s^{-1}); (e) k_1 180 s^{-1}; (f) k_1 410 s^{-1}.

complexes are fluxional at room temperature. When one of the two separate resonances observed for the COD olefinic protons (one for those *trans* to N, the other for those *trans* to O) at room temperature is irradiated, a large apparent, negative nOe (due to saturation transfer) is observed at the other resonance. Variable temperature studies of the Rh- and Ir-8hq complexes were carried out as mononuclear models for the binuclear hydroxypyridinate compounds.

Figure 9 shows the COD olefinic region in the ^{1}H NMR spectrum of [Rh(COD)(8hq)] in *o*-xylene-d_{10} as a function of temperature with the simulated spectra. Between 252 and 263 K, the line widths remained approximately constant, indicative of slow exchange. The spectra were modeled with the assumption that each resonance was a singlet, with a natural line width equal to the linewidth at 252 K [12*]. As the temperature is increased, the olefinic resonances broaden until at the highest temperature studied, 400 K, the olefinic resonances began to coalesce. The changes in the spectrum were fully reversible. The calculated rates and free energies of activation, $\Delta G^{\ddagger}$ are listed in Table 4. The calculated activation parameters are $\Delta H^{\ddagger} = 8.7 \pm 0.6$ kcal/mol and $\Delta S^{\ddagger} = -26 \pm 2$ e.u. [9].

A more limited variable temperature study of [Ir(COD)(8hq)] in *o*-xylene-d_{10} (five temperatures between 294 and 400 K) was also carried out. The spectra were simulated in the same manner as for the Rh complex, but a value of 10.0 Hz was

Table 4

Calculated rates and activation energies for proton exchange in [Rh(COD)(8hq)]

T (K)	k (s^{-1})	$\Delta G^{\ddagger}$ (kcal/mol)
252	–	–
285	1.75	16.3
297	9.66	16.0
303	5.80	16.7
331	44.6	16.9
359	98.5	17.9
378	152	18.5
390	177	19.0
400	409	18.9

Table 5

Calculated rates and activation energies for proton exchange in [Ir(COD)(8hq)]

T (K)	k (s^{-1})	$\Delta G^{\ddagger}$ (kcal/mol)
294	1.22	17.1
298	2.46	16.9
303	3.20	17.1
345	50.7	17.6
400	222	19.4

assumed (line width at 294 K 10.4 Hz) for the low temperature limit. The exchange rates were generally lower for Ir(COD)(8hq) than those of [Rh(COD)(8hq)] at comparable temperatures. The changes in the spectrum were fully reversible. The calculated rates and free energies of activation are listed in Table 5. The calculated activation parameters are $\Delta H^{\ddagger} = 10.4 \pm 0.8$ kcal/mol and $\Delta S^{\ddagger} = -21.9 \pm 2$ e.u. [9].

The activation parameters for Ir(COD)(8hq) are not as accurately determined because only two spectra were obtainable at rates fast enough to cause significant broadening of the olefinic resonances. There is no doubt, however, that the activation barrier is higher in Ir(COD)(8hq) than in the Rh analogue.

Effect of concentration on exchange rates

The $[Rh(COD)(\mu\text{-hp})]_2$ complex was studied at 4.3 mM concentration in addition to the study at 7.5 mM, which was used for the simulations. At every temperature studied, both concentrations yielded identical band shapes, and the chemical shifts and line widths were identical, within experimental error. 4.0 mM toluene-d_8 solution of $[Ir(COD)(\mu\text{-hp})]_2$ also gave band shapes and line widths (for those spectra run at comparable temperatures) that were similar to those found in the more complete experiment on a 14.0 mM solution. There is no significant concentration effect on the rates of the fluxional process observed for the Ir_2 complex or on either of the two processes observed for the Rh_2 complex.

Effect of added COD

The NMR spectrum of a sample of $[Ir(COD)(\mu\text{-Hp})]_2$ (22.0 mM) that contained free COD (10 mM) in toluene-d_8 was studied at five temperatures between 220 and

400 K [9]. The linewidth of the free COD olefinic resonance was 8.2 ± 0.2 Hz at all temperatures studied. The band shapes and linewidths of the Ir_2 complex resonances were unaffected by the presence of free COD. A similar experiment was carried out for [Rh(COD)(μ-hp)]$_2$ (26 m*M* in complex, 14 m*M* free COD), and again the free COD resonances did not broaden significantly at high temperature [9]. The resonances of the Rh_2 complex were unaffected, between 220 and 400 K, by the presence of free COD.

Effect of added acetonitrile

The effect of added nucleophile on the exchange rates for the hp complexes was evaluated by studies conducted as a function of temperature in the presence of CH_3CN. Samples containing 25 m*M* in [Rh(COD)(μ-hp)]$_2$ with 580 m*M* CH_3CN in toluene-d_8 and 22 m*M* [Ir(COD)(μ-hp)]$_2$ with 38 m*M* CH_3CN were studied at five temperatures between 220 and 400 K. There is no significant effect on the band shapes of the spectra of the hp complexes by CH_3CN at any temperature studied.

Variable temperature ^{1}H NMR spectrum of [Ir(COD)(μ-pz)]$_2$

The ^{1}H NMR spectrum of [Ir(COD)(μ-pz)]$_2$ in *o*-xylene-d_{10} was studied at 298, 349, and 396 K. No detectable broadening of the COD resonances is observed (line width of COD olefinic signals 16.6 ± 0.1 Hz at all three temperatures). These results indicate that there is no facile process in the pyrazolyl bridged complex that interconverts inside with outside COD protons on the NMR time scale, even at elevated temperatures. This result is consistent with previously reported experiments for the Rh_2 analogue, [Rh(COD)(μ-pz)]$_2$, where the ^{1}H NMR spectrum displayed broadening of the *endo*-methylene resonances only, at 383 K [13]. The small value of the chemical shift difference between inside and outside *endo*-methylene resonances in the Rh_2 complex of only 7.5 Hz (at 300 MHz), coupled with the observed slight broadening indicates a large activation barrier in the Rh_2 complex as well.

"Cross-over" experiments

Because the sodium salts of the free hydroxypyridinate anions are not soluble in toluene, we were not able to determine whether the coordinated hydroxypyridinate ligands would undergo exchange with free hydroxypyridinates. However, "cross-over" studies were feasible, and new species should be detected when two different hydroxypyridinate complexes are mixed together. Many different possible combinations of complexes are possible, and several were tried.

The Reaction of [Ir(COD)(μ-hp)]$_2$ with [Ir(COD)(μ-mhp)]$_2$

A toluene-d_8 solution of [Ir(COD)(μ-hp)]$_2$ (5.5 mg, 6.7×10^{-3} mmol) and [Ir(COD)(μ-mhp)]$_2$ (5.4 mg, 6.8×10^{-3} mmol) was prepared while closely monitoring the temperature of the sample. During its preparation, the sample was kept frozen at 77 K, then warmed to 195 K (in a CO_2/isopropanol bath) prior to insertion into the NMR probe, which had been cooled to 238 K. At 238 K, the spectrum showed only resonances due to [Ir(COD)(μ-hp)]$_2$ and [Ir(COD)(μ-mhp)]$_2$. The probe was maintained at this temperature for 6.3 h. Spectra were taken periodically and showed no evidence of the formation of a mixed bridge species. The probe temperature was gradually raised to 298 K and a spectrum was immediately taken. No spectral changes were observed [9]. After 15 min at 298 K, new

signals were apparent. After 3.5 h at 298 K, the solution contained a ca. 1/1/1 mixture of $[Ir(COD)(\mu\text{-hp})]_2$, $[Ir(COD)(\mu\text{-mhp})]_2$, and a new species, presumably $[Ir_2(COD)_2(\mu\text{-hp})(\mu\text{-mhp})]$.

In the spectrum of the mixture, the COD region is quite complicated, but the hydroxypyridinate signals clearly indicate that a single new species has been formed. A new mhp methyl singlet at 2.80 ppm (the methyl signal appears at 2.78 ppm in $[Ir(COD)(\mu\text{-mhp})]_2$ at this temperature) is due to the mixed bridge $[Ir_2(COD)_2(\mu\text{-hp})(\mu\text{-mhp})]$ complex. With the assumption that only "head-to-tail" structures are stable, there is a single chemically distinct mixed hp/mhp Ir_2 complex possible.

At 238 K, the half life of the process that interconverts *trans* to N with *trans* to O COD protons in $[Ir(COD)(\mu\text{-hp})]_2$ is 62 s. Even if the analogous process in the mhp complex is two orders of magnitude slower (100 min), more than ten half lives of the mhp complex elapsed at 238 K without the formation of the mixed bridge species. A lower limit on the half life of the second process (which interconverts inside and outside protons) in the $[Ir(COD)(\mu\text{-hp})]_2$ complex is estimated to be 8.8 h (the calculated value for $[Rh(COD)(\mu\text{-mhp})]_2$ at 238 K). At 298 K, the half life of the *trans* to N/*trans* to O interchange is 0.15 s. If the rate of the same process in the mhp complex is two orders of magnitude slower, four half lives would elapse in one minute, a rate much faster than the rate of the observed changes. A lower limit of the second process in $[Ir(COD)(\mu\text{-hp})]_2$ is 0.9 s (the value for the Rh_2 analogue). These experiments demonstrate that ligand exchange does not occur during or faster than process 1; further, they indicate that process 1 is intramolecular.

The reaction of $[Ir(COD)(\mu\text{-hp})]_2$ with $[Rh(COD)(\mu\text{-hp})]_2$

The 298 K spectrum [9] of a toluene-d_8 solution containing 7.7 mg of $[Ir(COD)(\mu\text{-hp})]_2$ (9.8×10^{-3} mmol) and 7.7 mg of $[Rh(COD))(\mu\text{-hp})]_2$ (1.3×10^{-2} mmol) was obtained. The sample was kept at room temperature in the dark, and the spectrum was recorded within a few hours of its preparation. The presence of a new species can be inferred from the COD olefinic region and from the signals due to proton H5, two sharp resonances superimposed on a broad signal. The sharp resonances at 7.98 and 8.00 ppm are due to $[Ir(COD)(\mu\text{-hp})]_2$ and $[Rh(COD)(\mu\text{-hp})]_2$, respectively. At 210 K, the broad H5 signal collapses to two doublets, giving a total of four different H5 resonances. The outer doublets at 8.25 and 8.00 ppm are of approximately equal intensity and are due to the new compound. Again, if only head to tail isomers are stable, there is only one possible new species, $[IrRh(COD)_2(\mu\text{-hp})_2]$. The mixed metal complex presumably has C_s symmetry with two chemically non-equivalent, bridging hp ligands. At 298 K, the fluxional processes in the mixed metal species are more rapid than in either the Ir_2 or Rh_2 complexes. After heating to 390 K, the relative proportion of the mixed metal complex at 298 K was approximately the same as before heating.

A second experiment was carried out with a mixture of $[Ir(COD)(\mu\text{-hp})]_2$ (5.7 mg, 7.2×10^{-3} mmol) and $[Rh(COD)(\mu\text{-hp})]_2$ (4.7 mg, 7.7×10^{-3} mmol) in toluene-d_8, with careful monitoring of the temperature of the sample. The sample was kept frozen at 77 K during its preparation, then warmed to 195 K with a CO_2/isopropanol bath prior to insertion into the NMR probe (cooled to 206 K). The probe was warmed to 220 K, and spectra were run over a 3 h period. During this time, the resonances of the Rh_2 complex grew in as the compound dissolved, but no other changes occurred. The temperature was raised to 240 K, and spectra

were run over a 1 h period. Again, no new species were observed. While holding the sample above 265 K for 100 min, the resonances due to the mixed metal complex grew in. After heating to 325 K, the probe was cooled to 265 K, and the spectrum was taken. The resonances due to the mixed metal compound grew in during this time (approximately 45 min).

At 220 K, the half life of the process that interconverts *trans* to N with *trans* to O COD protons (process 1) is 11 min for M = Ir and 0.62 s for M = Rh. After 3 h, or 16 half lives of process 1 in the Ir_2 complex and 17000 half lives of process 1 in the Rh_2 complex, no mixed metal species was formed. The half life of the process that interconverts inside with outside COD protons (process 2) is 7.1 weeks for M = Rh and much longer for M = Ir. At 240 K, process 1 has a half life of 45 s for the Ir_2 complex and 0.069 s for the Rh_2 complex. After 1 h at 240 K, 45 half lives of process 1 in the Ir_2 complex and 52000 half lives of process 1 in the Rh_2 complex elapsed, and no mixed metal complex was formed. Process 2 has a half life of 8.8 h at this temperature (M = Rh) and again, much longer for M = Ir. Above 265 K, the rate of the inside/outside process becomes more rapid in the Rh_2 complex (half life 3.2 min at 265 K). This second process may be responsible for the observed formation of the mixed metal species. The slow growth of the mixed metal resonances after heating the sample to 325 K (a temperature where process 1 occurs quite rapidly in both complexes) further demonstrates that the *trans* to N/*trans* to O interconversion (process 1) is unrelated to the chemical reaction that scrambles the metals.

The reaction of [Rh(COD)(μ-hp)]$_2$ with [Rh(COD)(μ-mhp)]$_2$

The 200 K spectrum of a mixture of [Rh(COD)(μ-mhp)]$_2$ (6.5 mg, 1.0×10^{-2} mmol) and [Rh(COD)(μ-hp)]$_2$ (6.3 mg, 1.0×10^{-2} mmol) in toluene-d_8 was obtained. The solution was kept at room temperature in the dark and run within a few hours of preparation. As in the case of the Ir_2 analogues, a new mhp methyl resonance at 3.03 ppm and a new H5 resonance at 8.20 ppm indicate the formation of [Rh_2(COD)$_2$(μ-hp)(μ-mhp)]. No further studies were carried out on this solution.

The reaction of [Ir(COD)(μ-mhp)]$_2$ with [Rh(COD)(μ-mhp)]$_2$

The 200 K spectrum [9] of a mixture of [Ir(COD)(μ-mhp)]$_2$ (7.0 mg, 8.6×10^{-3} mmol) and [Rh(COD)(μ-mhp)]$_2$ (6.4 mg, 1.0×10^{-2} mmol) in toluene-d_8 was obtained. The solution was kept at room temperature in the dark and run within a few hours of preparation. An additional mhp methyl resonance at 2.79 ppm as well as new COD olefinic resonances are consistent with the formation of the mixed metal species [IrRh(COD)$_2$(μ-mhp)$_2$]. No further studies were carried out with this solution.

Discussion

There have been several variable temperature NMR studies of mononuclear square planar complexes that contain dienes. Vrieze and coworkers [14] have studied the behavior of [M(diene)(L)Cl], where M = Rh and Ir, diene = COD and norbornadiene (NBD) and L = PPh_3 and $AsPh_3$ in the absence and presence of free L, diene, and binuclear [Rh(diene)Cl]$_2$. The results of these studies showed that ligand dissociation and intermolecular reactions were the source of the diene signal

Table 6

Activation parameters of $[M(COD)(\mu\text{-hp})]_2$ and [M(COD)(8hq)]

Compound	$\Delta H^{\ddagger}$ (kcal/mol)	$\Delta S^{\ddagger}$ (e.u.)	$\Delta G^{\ddagger}$ (298) [a] (kcal/mol)
$[Ir(COD)(\mu\text{-hp})]_2$ (1)	13.5 ± 0.8	-10.2 ± 2.0	16.5
(2)	– [b]	– [b]	> 20.5 [c]
$[Rh(COD)(\mu\text{-hp})]_2$ (1)	11.1 ± 0.1	-7.4 ± 0.4	13.3
(2)	25.3 ± 1.0	25.9 ± 4.0	17.6
[Ir(COD)(8hq)]	10.4 ± 0.8	-21.9 ± 2.0	16.9
[Rh(COD)(8hq)]	8.7 ± 0.7	-25.8 ± 2.0	16.5
[Rh(COD)(sbdm)] [d]	10.5 ± 0.5 [e]	−20.9 [f,g]	16.7
$[(Rh(COD))_2(salophen)]$ [h]	11.4 [e,g]	−19.0 [f,g]	17.1

[a] $\Delta G^{\ddagger}(298) = \Delta H^{\ddagger} - 298(\Delta S^{\ddagger})$. [b] The rate of process 2 in $[Ir(COD)(\mu\text{-hp})]_2$ is too slow to measure between 200 and 400 K. [c] A lower limit assuming an upper limit of 50 s^{-1} for process 2. [d] Ref. 7, in $o\text{-}C_6H_4Cl_2$ in presence of 1.25 equiv. $AsPPh_3$. [e] Estimated from reported E_a using $\Delta H^{\ddagger} = E_a - RT$, T 298 K. [f] Estimated from reported A factor using $\Delta S^{\ddagger} = R[\ln(A/T) - \ln(e^2 k_b/h)]$, T 298 K. [g] Error limits not reported. [h] Ref. 4, in CD_5Cl.

averaging. An associative mechanism that involved the formation of five-coordinate intermediates was postulated to account for the observed behavior.

Lippard and Heitner [15] have studied compounds of the form [Rh(diene)(L)], where L are various monothio-diketonates. As in the previous case, an associative mechanism, with the formation of a five-coordinate intermediate, was postulated, where the fifth ligand was an added nucleophile or the solvent (nitrobenzene or *o*-dichlorobenzene). The Arrhenius activation parameters measured by these workers are listed in Table 6. The Arrhenius activation energies, particularly for [Rh(COD)(SBDM)] [16*], are quite in line with the $\Delta G^{\ddagger}$ we calculate for both [Ir(COD)(8hq)] and [Rh(COD)(8hq)] complexes. In addition, the negative $\Delta S^{\ddagger}$ observed for both complexes is consistent with the associative mechanism observed by Vrieze and Lippard et al. The fluxional rearrangements in the binuclear complexes are quite different than those observed for the mononuclear complexes.

It is clear that a single fluxional process in which *trans* to N COD atoms exchange with *trans* to O COD atoms but with the retention of the "inside–outside" stereochemistry is required to satisfactorily explain the spectral changes that occur in the Ir_2 complexes between 200 and 400 K. This will be called " process 1" and is so referred to in Table 6. An identical process occurs in the Rh_2 complexes, but with a lower activation barrier. In the Rh_2 complexes, a second process, that interconverts inside and outside COD atoms, is required to explain the spectral changes that occur at higher temperatures. We refer to this process as "process 2". Process 2 undoubtedly occurs in the Ir_2 complexes as some line shape changes occur, but at rates too slow to be accurately measured and at temperatures beyond the capability of our NMR equipment. An upper limit for k_2 in $[Ir(COD)(\mu\text{-hp})]_2$ at 400 K is 50 s^{-1} ($\Delta G^{\ddagger}$ 20.5 kcal/mol). It should be noted that the slowest rate that could accurately be measured by the line broadening technique was about 3 s^{-1}.

The low symmetry of the binuclear complexes combined with the previous, unambiguous assignment of the COD proton resonances [1b] allows several important conclusions to be drawn about processes 1 and 2.

Process 1

The permutation that describes the effect of process 1 on the olefinic protons is (11,16)(12,15). This eliminates from consideration a rotation of the COD ligand, i.e. a pathway involving a tetrahedral intermediate (permutation (11,15)(12,16), Table 1). Also eliminated is a process in which the conformation of the $(MNCO)_2$ 8-membered ring is inverted (a tub ↔ tub interconversion). This process interconverts inside and outside protons without exchanging *trans* to N and *trans* to O protons, and is described by the permutation (11,12)(15,16).

Process 1 does not interconvert *exo*- and *endo*-methylene protons. Process 1 does not involve full or partial COD ligand dissociation. Once dissociated, the COD ring would be free to undergo inversion as the activation barriers for the various interconversion processes available for free COD (twist, boat, chair, etc.) at 298 K, are at most 6.2 kcal/mol [17], far smaller than the barriers observed in this study. The inert nature of the COD ligand in these complexes is also supported by the lack of effect on the NMR spectra in the presence of free COD for the Ir_2 and Rh_2 compounds. Process 1 does not involve the breakage of the M–COD bonds.

Process 1 is probably not the result of the solvent assisted, associative pathway, which involves a five coordinate intermediate or transition state, commonly observed in substitution reactions of square planar 16 electron complexes [18]. In contrast, the mononuclear analogues we have studied ([Rh(COD)(8hq)] and [Ir(COD)(8hq)]) both have large activation enthalpies and large, negative activation entropies which suggest an associative type mechanism. These observed activation parameters are similar to the other square planar compounds containing COD ligands previously studied [7,15]. The considerably less negative activation entropies observed in the binuclear complexes, and the observed lack of a dependence on added acetonitrile rules out the mononuclear associative pathway for process 1.

We are unable to propose a chemically reasonable COD motion that can account for the observed exchange pattern in process 1, and propose a mechanism that involves motion of the bridging ligands. Because process 1 is strictly intramolecular (cf. the cross-over experiments with $[Ir(COD)(\mu\text{-hp})]_2$ and $[Rh(COD)(\mu\text{-hp})]_2$, and the inside and outside protons do not interconvert), the binuclearity and stereochemistry of the complexes must be preserved during Process 1. It is difficult to envision a mechanism that both accomplishes the required topological changes and preserves the inside-outside asymmetry, without breaking a M–N or M–O bond. A simple, concerted "end for end" flip of the bridging ligands (the long arrow shown in Fig. 10a) exchanges the correct protons. Another, more likely, mechanism that achieves this result is shown schematically as pathway A, B, C, D, C′, B′, A′ in Fig. 10. Step A involves the breaking of a M–N or M–O bond. We favor the breaking of the M–N bond for two reasons. Species that contain a "dangling", formally negatively charged oxygen should be strongly disfavored in a non-polar solvent such as toluene, and the M–N bond distances determined previously [1b] in $[M(COD)(\mu\text{-mhp})]_2$ are significantly longer and perhaps weaker than the M–O distances (an average of 0.064 Å for M = Ir (8 s.d.) and 0.053 Å for M = Rh (18 s.d.). Step B is the nucleophilic attack of the uncoordinated N on the same metal to form a chelated species with the other N uncoordinated. Reassociation of this second pyridine function to the other metal atom (step C) forms a doubly chelated species. The existence of $Ir(COD)(hp)(X)_2$, X = Cl, Br, I complexes [1a] that contain chelating hp ligands supports this possibility. Finally, the chelated metal centers

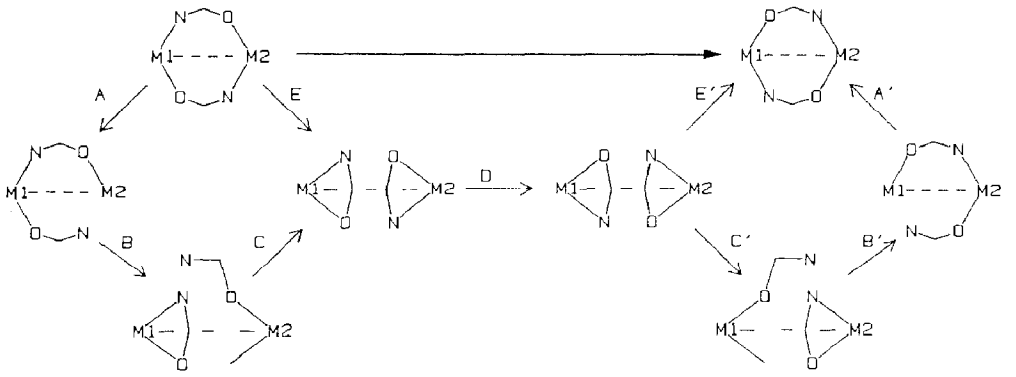

Fig. 10. Proposed mechanism for process 1. Only the relevant connectivities of the hp ligands are shown. The long arrow represents the net interconversion via a concerted process. Steps A, B, C, D and their primed analogues represent possible mechanistic steps along the reaction coordinate.

rearrange via two, sequential hp ligand rotations (Step D), followed by the reverse of Steps C, B, and A. There are less likely physical motions possible but only those that preserve the M–M interaction, the binuclearity and the inside–outside asymmetry of the COD ligands are consistent with all the data. It should be noted that any degree of rotation about the M–M "bond" also preserves the inside–outside asymmetry.

Process 2

Process 2 interconverts inside and outside protons, and is not affected by the presence of added COD, added acetonitrile, or the concentration of the metal complex. As for process 1, solvent assisted pathways and those that involve the dissociation of COD need not be considered. Allowed motions for this process include COD rotation through a tetrahedral geometry (Fig. 11A) at the metal center in the transition state or inversion of the $[MNCO]_2$ (Figure 11B) perhaps via a "crown conformation" in the transition state [18*].

Both of these mechanisms would require significant lengthening of the M–M interaction. For the rotation mechanism [20], X-ray structural data reveals that the significant ground state steric interactions between the two COD ligands would require substantial M–M bond lengthening to attain the pseudotetrahedral geometry required for the COD rotation mechanism. Similarly, the ring inversion mechanism entails an even larger lengthening of the metal–metal bond to the point of cleavage in the "crown" transition state. Thus, the large positive entropy of activation for process 2 in $[Rh(COD)(\mu\text{-hp})]_2$, which is suggestive of a highly dissociated transition state with considerable bond breaking, is consistent with either mechanism. The observed enthalpy of activation of 25.3 kcal/mol is also in line with breakage of the $Rh^{I}Rh^{I}$ interaction that has been estimated at 18 kcal/mol in $[Rh_2(bridge)_4]^{2+}$, a face-to-face d^8–d^8 complex [21]. The increased activation energy observed for the Ir analog also accords well with the expected increase in the strength of the Ir–Ir interaction as compared with the Rh–Rh interaction.

In principle, the COD rotation and the ring inversion mechanisms should not result in the scrambling observed in the cross-over reactions, but either of these mechanisms in combination with the rapid metal–ligand bond breakage from process 1 could result in the production of short lived, monuclear intermediates

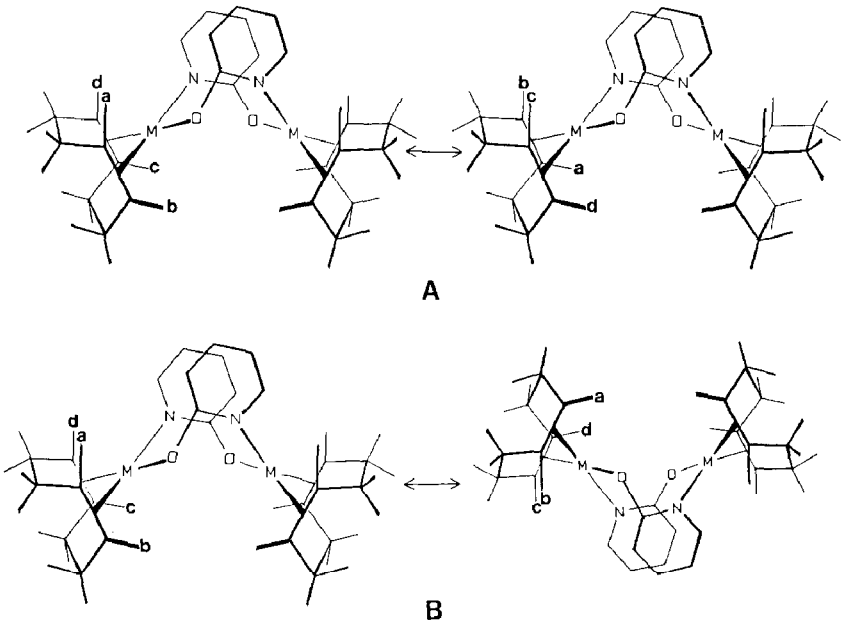

Fig. 11. Schematic diagram of the olefinic proton permutations for process 2. (A) COD ligand rotation (permutation (11,15)(12,16)) and (B) $[IrNCO]_2$ ring inversion (permutation (11,12)(15,16)). In this diagram a, b, c, and d initially correspond to hydrogens 12, 11, 15, and 16 respectively.

[22*]. The recombination of two intermediates from different binuclear complexes would account for all the observed cross-over products [23*].

Conclusions

Two distinct exchange processes interconvert non-equivalent COD protons in $[Rh(COD)(\mu\text{-hp})]_2$, but only the lower energy process is observed by ^1H NMR line broadening in $[Ir(COD)(\mu\text{-hp})]_2$. Their nature and activation parameters suggest that they are both significantly different from related processes observed in mononuclear Rh^I and Ir^I COD complexes. The lower energy process (process 1) retains the M–M interaction and involves the intramolecular head-to-tail exchange of the μ-hp ligands. Breakage of the M–N bond is suggested as the rate limiting step. The mechanism of the second intramolecular process that occurs at higher temperatures was not unambiguously determined but either consists of an inversion of the complex through a crown intermediate or a rotation of the COD ligands through a

Table 7

Correlation of M–M distance, λ_{max} for the $d\sigma^* \rightarrow p\sigma$ [b] absorption and $\Delta G^{\ddagger}$ for process 2

Complex	M–M distance [a] (Å)	$\lambda_{max}\, d\sigma^* \rightarrow p\sigma$ [b] (cm^{-1})	$\Delta G^{\ddagger}(298)$ [c] (kcal/mol)
$[Ir(COD)(\mu\text{-hp})]_2$	3.242	20400	> 20.5
$[Rh(COD)(\mu\text{-hp})]_2$	3.367	23700	17.6

[a] Crystallographic data collected for the mhp complexes. [b] A smaller transition energy implies a stronger M–M interaction. [c] Free energy of activation for process 2.

tetrahedral transition state. Both mechanisms have a considerable energy contribution from the breakage of the M–M interaction; and as expected, based on trends in M–M bonding, the second process is slower for M = Ir than for M = Rh. Table 7 summarizes the relationship between M–M distance, λ_{max} for the $d\sigma^* \rightarrow p\sigma$ electronic transition and the $\Delta G^{\ddagger}$ for process 2. Finally, it is of interest that the simultaneous occurrence of both intramolecular processes at the highest temperatures studied leads to intermolecular ligand and metal scrambling, as indicated by cross-over experiments.

Supplementary material available:

$\Delta G^{\ddagger}$ vs. T plots for Ir(COD)(μ-hp), Rh(COD)(8hq) and Ir(COD)(8hq); simulated and observed ^{1}H NMR spectra of $[Rh(COD)(\mu\text{-hp})]_2$, $[Ir(COD)(\mu\text{-hp})]_2$ + COD, $[Rh(COD)(\mu\text{-hp})]_2$ + COD, $[Ir(COD)(\mu\text{-hp})]_2$ + $[Ir(COD)(\mu\text{-mhp})]_2$ and $[Ir(COD)(\mu\text{-hp})]_2$ + $[Rh(COD)(\mu\text{-hp})]_2$. Ordering information can be obtained from the authors.

Acknowledgement:

We wish to thank Dr. Richard Newmark for valuable discussions and Johnson–Matthey, Inc. for a loan of rhodium and iridium trichloride.

References

1 (a) G.S. Rodman, K.R. Mann, Inorg. Chem., 24 (1985) 3507; (b) 27 (188) 3388.
2 T. Sielisch, M. Cowie, Organometallics, 7 (1988) 707.
3 K.A. Beveridge, G.W. Bushnell, S.R. Stobart, J.L. Atwood, M.J. Zaworothko, Organometallics, (1983) 1447.
4 (a) A.L. Van Geet, Anal. Chem., 42 (1970) 679; (b) 40 (1968) 2227.
5 P. Meakin, E.L. Meuterties, F.N. Tebbe, J.P. Jesson, J. Am. Chem. Soc., 93 (1971) 4701.
6 R.B. King, Inorg. Chem., 20 (1981) 363.
7 R. Bonnaire, J.M. Manoli, C. Potvin, N. Platzer, N. Goasdoue, D. Davoust, Inorg. Chem., 21 (1982) 2032.
8 The use of two dummy spins introduces a source of error in the calculations, because the olefinic protons actually couple to six different methylene protons (two olefinic methylene-proton coupling constants are negligible). The simulation program could not handle the complete ten spin problem. The error associated with this approximation should be small at low temperatures, where the rates are slow, and at moderate temperatures, where the line widths are quite broad and not very sensitive to the artificially increased number of connected transitions. At the highest temperature observed (400 K), the line width of the overlapping COD signals is 82 Hz, still broad enough so that the six spin approximation is expected to yield reasonable results. The natural line width was approximated at 1.75 Hz based on the static simulation at room temperature. Because the spectrum of the complex contains no singlet resonances, the natural line width was not readily determined, and is a source of systematic error.
9 Included as Supplementary Material.
10 The coupling constants derived from the static simulation of the Ir_2 complex were modified where necessary to simulate the Rh_2 complex in the stopped exchange region. The six spin approximation broke down at the two highest temperatures studied, 382 and 402 K, because the experimentally observed line widths became so narrow that the effect of artificially increasing the number of connected transitions was no longer negligible. The natural line width was approximated to be 5.0 Hz based on the static simulation at 223 K. Again, this is a source of systematic error in the calculations.
11 R. Ugo, G. La Monica, S. Cenini, F. Bonati, J. Organomet. Chem., 11 (1968) 159.
12 Neglecting the coupling in the COD ligand introduces some systematic error into the rate calculations. However, because the lines are quite broad in the region studied (width at 252 K, 10.8 Hz, width at 400 K > 140 Hz), this source of error is not important.

13 J. Elguero, M. Esteban, M.F. Grenier-Loustalot, L.A. Oro, M.T. Pinilos, J. Chim. Phys. Phys.-Chim. Biol., 81 (1984) 251.
14 K. Vrieze, P.W.N.M. van Leeuwen, Prog. Inorg. Chem., 14 (1971) 1 and ref. therein.
15 (a) H.L. Heitner, S.J. Lippard, J. Am. Chem. Soc., 92 (1970) 3486; (b) H.L. Heitner, S.J. Lippard, Inorg. Chem., 11 (1972) 1447.
16 The ligand SBDM = $[SC(Ph)CHC(Ph)O]^-$.
17 (a) O. Ermer, J. Am. Chem. Soc., 98 (1976) 3964; (b) F.A.L. Anet, L. Kozerski, ibid., 95 (1973) 3407.
18 J.D. Atwood, Inorganic and Organometallic Reaction Mechanisms, Brooks/Cole Publishing Company, Monterey, CA, 1985.
19 An energetically less likely but allowed alternative is the complete dissociation of the bridging ligands followed by breakage of the M–M bond to produce mononuclear species.
20 (a) R. Hill, B.A. Kelly, F.G. Kennedy, S.A.R. Knox, P. Woodward, J. Chem. Soc. Chem. Commun., (1977) 434; (b) M.J. Chem, H.M. Feder, Inorg. Chem., 18 (1979) 1864.
21 S.F. Rice, H.B. Gray, J. Am. Chem. Soc., 103 (1981) 1595.
22 The exact relationship of cross-over product formation to process 2 is a question of interest. Experimental difficulties have precluded the direct measurement of the rate for any of the cross-over reactions, but in any event, the rates are not faster than the rate of process 2. The observation of cross-over rates slower than process 2 with a second order concentration dependence would be additional evidence for our proposed mechanism.
23 The concentration of mononuclear intermediates (if they are in fact present in bulk solution) is small. The chemical shifts of the coalesced lines at higher temperatures are within experimental error of the appropriate average of the calculated static chemical shifts. Variable temperature UV-Vis absorption measurements [24] are also consistent with at most a very low bulk concentration of mononuclear species.
24 G.S. Rodman, Ph.D. Thesis, University of Minnesota, 1987.